Tikrit Journal of Pure Science
ISSN: 1813 – 1662 (Print) --- E-ISSN: 2415 – 1726 (Online)
Journal Homepage: http://tjps.tu.edu.iq/index.php/j

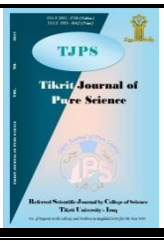

Reservoir Characteristics of the Lower Miocene Carbonate Formations in Kor Mor Gasfield, Kirkuk Area, NE Iraq

Fouad M. Qader, Shabaz M. Ali
Geology Department, College of Science, University of Sulaimani, Sulaimani, Iraq

https://doi.org/10.25130/tjps.v27i3.52

ARTICLE INFO.

Article history:

-Received:	**15 / 4 / 2022**
-Received in revised form:	**8 / 5 / 2022**
-Accepted:	**14 / 6 / 2022**
-Final Proofreading:	**12 / 7 / 2022**
-Available online:	**28 / 7 / 2022**

Keywords: Kor Mor Field, Reservoir Characterization, Euphrates, and Jeribe formations.

Corresponding Author:
Name: Fouad M. Qader
E-mail: fuad.qadir@univsul.edu.iq
Tel:

ABSTRACT

This paper presents the evaluations of the reservoir characterization of the Lower Miocene Euphrates, and Jeribe carbonate formations selected for this study in Kor Mor Gasfield in Northeastern Iraq. The thickness of Euphrates ranges between 30 and 65m, and Jeribe between 30 and 50m in this field. They are overlain by a thick evaporate cap rock of the Fatha Formation. The two formations are separated by the thin evaporate rock unit of the Dhiban Formation. The full set of log data for the well Km-9 was used in addition to some general data derived from other eight wells (Km-1 to Km-8). The log data was used in evaluating the reservoir properties of the two rock units. The detected lithologies from the available mud log and well reports showed that the two formations, mostly dolostone and dolomitic limestone, were dominated. From the log data, different reservoir properties including clay content, clay types, porosity, and fracture index were estimated. The average porosity of the Euphrates reservoir was around 0.15 and that of the Jeribe was about 0.10. The secondary porosity made a significant fraction of porosity in both units.

1. Introduction

The Kor Mor Field is located in the NE part of Iraq. The Field lies 35 Km to the southeastern part of Kirkuk City and about 8 Km to the southwestern part of Qadir-Karam Town (Fig. 1). The structure was firstly discovered in 1927 by Iraq Petroleum Company (IPC) during a general geological survey in the northern part of Iraq. This study is based on the importance of the carbonate successions in the Upper Oligocene and Lower Miocene since Iraq's Cenozoic sequence has about 16 percent of the country's oil reserves [1]. Numerous authors in many parts of Iraq have studied the Lower Miocene units. Some of those authors during the last decade, who focused on the reservoir characteristics in central and north areas, included Al-Ameri et al. [2]; Hussein [3]; Baban et al. [4]; Hussein et al. [5]; Saeed [6]; Abdullah et al. [7]; Fadhil et al. [8]; Abdulrahman et al. [9]; and Deabl et al. [10]. The goal of this study is to investigate the reservoir characteristics of the Lower Miocene Jeribe and Euphrates formations in Kor Mor Field.

The first explored well (Km-1) was drilled in 1928, on the middle of the SW flank of the structure by (IPC) to discover the Hydrocarbon potential of the structure to the TD 1971.6 m RT in Jeribe Formation [11]. The well proved the existence of gas in the Jeribe Formation (previously called the Main limestone). The well Km-2 was drilled in 1952 at NE flank to the total depth of 1614 m RT in Jeribe Formation. The well-completion test proved the presence of gas in the Jeribe Formation [11].

The wells (3 to 8) were drilled during the period (1980-1990) by (NOC) as a development plan to produce gas with condensates from the field to provide the south Jambur degassing station. The well of Km-3 (the deepest exploration and evaluation of the well in the field) was drilled at the NE flank toward the NW plunge of the field to explore the possibilities of hydrocarbon in Cretaceous formations. The well reached the TD of 2962m in Kometan formation. The test results proved that the Upper Cretaceous reservoirs were dry [11].

In 2008, DanaGas/ Crescent Petroleum Company has delineated the structure by using a (2D) seismic survey made by Tera-Sise Canadian Company. Depending on the seismic results, the location of the well Km-9 has been drilled. The well has two targets, the primary one is to explore the Cretaceous formations, and the second target is to produce gas from Tertiary reservoirs. The drilling was spaded on Jan. 25th /2009, the final TD of the well (3054 m RTKB) was in Balambo formation [12].

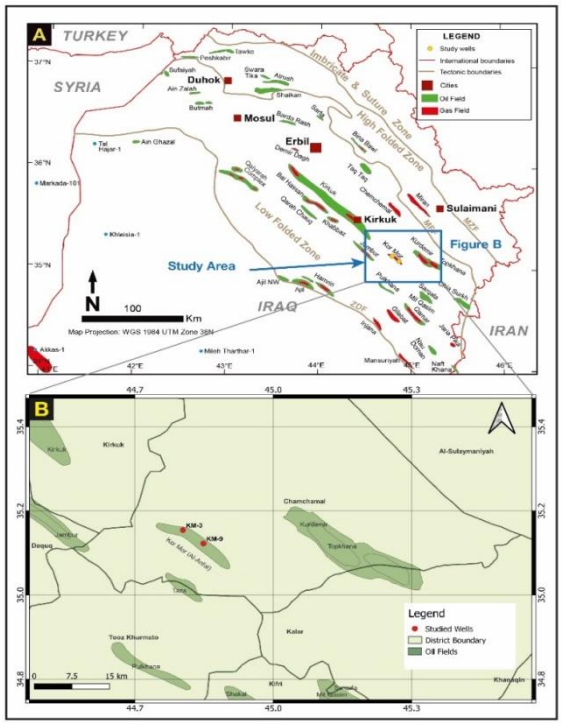

Fig. 1: (A) Map of Iraq showing structural provinces and (B) the location of the Kor Mor Field [13, 14]

2. Materials and Methods

The main tools used in this study were different types of logs, namely: Gamma Ray, Gamma Ray Spectrometry, Caliper Log, Neutron Log, Density Log, and Sonic Log in the well of Km-9.

Before starting the interpretation, the log data were corrected from shale content. Later, the TechLog software was utilized to adjust the environmental situation and analyze the well logs.

In addition, other available subsurface data from wells of Km-1 to Km-9 were used [11, 12]. These data included high pressure zone (Gas Kick), low pressure zone (mud loss), rate of penetration, rock properties obtained from mud log, and final well reports. They were used in calibrating the outputs of the log analysis.

3. Geological Setting

The Kor Mor field is the SE extension of Kirkuk Structure, which is separated by a saddle about (20) Km in length. This field is a huge gas field, the production is from the Tertiary reservoirs (Jeribe and the Euphrates), which are the gas reservoirs in many fields in the area (for example, Jambur and Hamreen), in addition to the documented oil in Lower Fars (Fatha formation) [11]. According to the tectonic classification of Iraq [13], the field locates in Foot-Hill Zone, Makhul-Hemrin Subzone (Kirkuk Embayment) that belongs to the Unstable Shelf.

The Kor Mor structure is (35) Km long and (5) Km wide, with an asymmetrical anticline. Its northeast flank is less inclined than its southwest one. The dip on the (SW) flank is (30^0), while the dip to the (NE) flank is (15^0) (Fig. 2). According to the seismic investigation of the area done by the Iraqi Petroleum Company in 1955, it indicated a subsurface structure plunging toward the northwest. In addition, two major faults intersected the structure to the SE plunge and SW limb, with having a significant influence on reservoir performance [12].

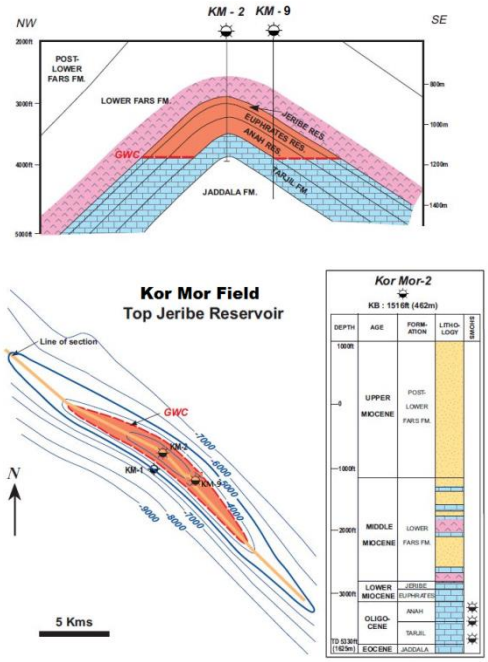

Fig. 2: Schematic cross section of Kor Mor Field, structural map of the top of Jeribe reservoir and stratigraphic column of the field [15]

3.1 Stratigraphy and Lithology

The Miocene succession in Iraq is represented by the Ghar, Serikagni, Euphrates, Dhiban, and Jeribe formations in the Lower Miocene; while the Fatha, Injana, Mukdadiya, and Bai Hassan formations in the Middle-Upper Miocene [13].

The Lower Miocene units in Iraq represent deepwater facies of the Serikagni formation (basinal), shallow carbonate, and evaporate facies of the Euphrates, Dhiban, and Jeribe formations [16].

The Jeribe and Euphrates formations in Lower Miocene are considered as significant reservoirs. They contain oil and gas in excess of 30 structures in Iraq. Most of the production comes from Jeribe and Euphrates formations in most fields in Iraq, particularly the northern ones [17].

The Kor Mor area is covered by thick layers of Upper Fars (Injanah) and Lower Fars (Fatha) formations

before getting the Jeribe, Dhiban, Euphrates, and Anah-Azkand formations.

3.1.1 Jeribe Formation

In 1957, Bellen defined and described the Jeribe limestone formation as of the type locality near Jaddala Village in Jebel Sinjar [18], and it is thought to be of Early Miocene age. Then, Damesin defined this formation in 1963 in an unpublished report.

The thickness in the type locality is around 73m and is mainly composed of massive recrystallized and dolomitized limestone, with beds of 1-2m thick [18]. Jeribe formation is equivalent to Govanda Limestone formation in age.

The formation, however, has been included into the Middle Miocene Sequence, due to the presence of the *Orbulina* datum towards the base of Jeribe formation [19]. According to the depositional environment study in the Azh Dagh-Qara Wais anticline, the Jeribe formation is deposited in a hypersaline lagoon to a restricted lagoon [7].

The thickness of the Jeribe formation in the Kor Mor field is ranged between 30 and 50m all over the drilled wells [11]. The formation is comprised of a series of brown to grey recrystallized dolostone with dolomitic limestone and anhydrite nodules. According to the final well report [12], severe mud losses and gas flow have been encountered while drilling the formation due to the fractures and vugs. This formation underlies Dhiban anhydrite formation with a thickness of 3 to 10 m in the drilled wells [11].

3.1.2 Euphrates Formation

It was first described by De Böckh [20] and then revised by Bellen in 1957 [18]. The type-site on the Stable Shelf in Wadi Fuhaimi near Anah consists of 8m of shelly, chalky, and well-bedded recrystallized limestone. Nevertheless, this limestone represents only a small section of the formation and does not include the basal conglomerate. Sands and anhydrite are also found in some subsurface layers [18] and are thought to be tongues of the Ghar and Dhiban formations [17].

According to the depositional environments study [7], the Euphrates formation passes up from deposits of restricted lagoon to shoal depositional environments.

The thickness of Euphrates formation in Kor Mor field is ranged between 30 and 65m in wells of Km-2, 3, 7, and 9 [11]. Consistent with this report [12], this formation consists of a thin sequence of brown dolomitic limestone and marly limestone affected by the diagenesis with secondary anhydrite nodules. In addition, oil stains, bitumen and gas are observed along the upper part of the formation, as well as mud losses are reported during drilling [12].

4. Results and Discussion

4.1 Shale Volume Calculation

Gamma ray logging is often regarded as the most effective method for finding shales within logged intervals. That is why gamma ray log is occasionally referred to as "shale log" [21].

Due to the fact that radiation strength is proportional to the amount of radioactive materials present, the gamma ray recorded by the tool's detector in API units can be converted to shale volume as a fraction or percentage.

Shale volume was computed for the Jeribe and Euphrates formations using data from the gamma ray log and the equation of the gamma ray index (Eq. 1) [22], shale volume calculation of Tertiary equation rocks (Eq. 2), [23].

$$IGR=\frac{GRlog-GRmin}{GRmax-GRmin} \quad \ldots\ldots\ldots \text{Eq. 1.}$$

Where IGR is gamma ray index, GR_{log} is gamma ray recorded value at any depth (in API), GR_{min} is minimum gamma ray recorded value at clean (non-shale) zone (in API), GR_{max} is maximum gamma ray recorded value at shale zone (in API).

$$Vsh = 0.083[2^{3.7.IGR} - 1] \quad \ldots\ldots\ldots \text{Eq. 2.}$$

According to [24], reservoir rocks are classified based on the percentage of shale or shale volume (V_{sh}) into: clean zone (V_{sh}<10 %), shaly zone (V_{sh}10 – 35%), and shale zone (V_{sh}> 35 %).

The determined volume of shale as seen in the upper part of the Jeribe formation (Fig.3) contained higher shale contents than the other parts, especially some intervals of its upper part (1241-1249m and 1256-1260m). These parts are mostly shaly dominants, while its lower part from the depth range (1260-1276m) to the lower boundary with Dhiban formation is clean zone.

Dhiban formation (interval 1276m to 1279.5m) is anhydrite, and it is excluded from further analysis. Regarding the Euphrates formation, its upper part is characterized by lower shale contents, except two beds in the depths 1282m and 1285.5m (Fig.3); while the lower part (1301-1311m) is characterized by high shale contents.

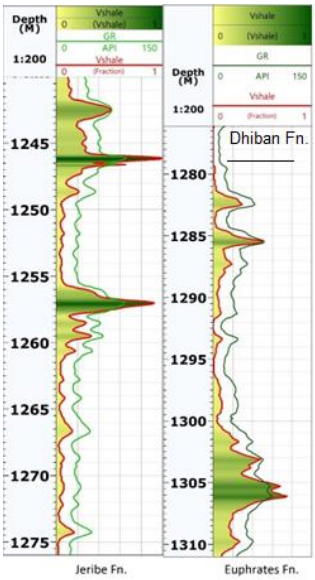

Fig. 3: Gamma ray log and the calculated shale volume for the Jeribe and Euphrates formations at the studied well

4.2 Natural Gamma Ray Spectroscopy

In this study, the data of the natural gamma ray spectroscopy was available for Jeribe, Dhiban, and Euphrates formations at the well of Km-9. Natural Gamma Ray Spectroscopy measures the mass concentrations of uranium (U), thorium (Th), and potassium (K) independently. This tool is used to identify clay mineral in reservoir rocks, which is helpful to the evaluation of reservoir through applying special crossplots and graphs established to be used for such a purpose. The Th/K crossplot (Fig.4) shows that most of the clay minerals forming the shale content consist of Glauconite, Illite, and Micas with a little contribution from other kinds of clay minerals like Montmorillonite. This indicates the effect of the basinal depositional environments on the Jeribe and Euphrates formations [25].

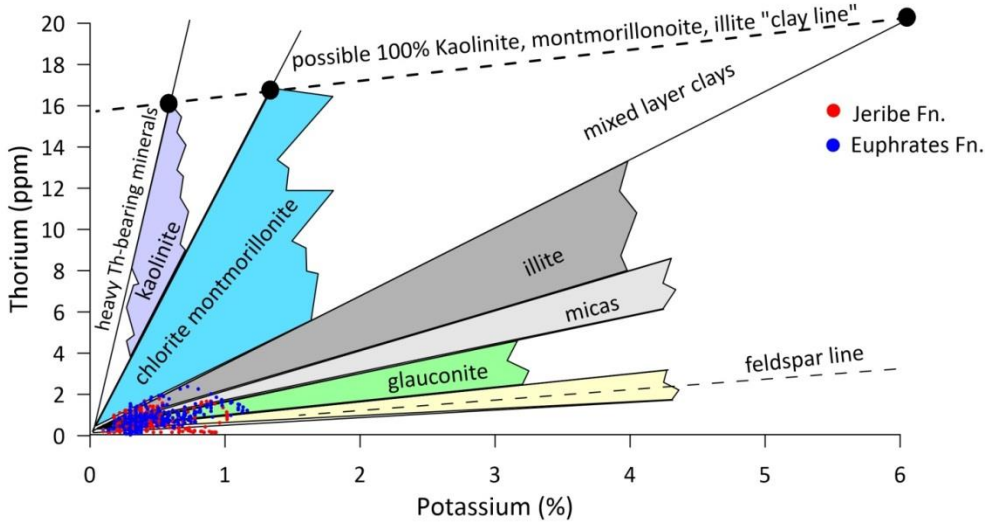

Fig. 4: The Th/K chart showing clay types in Jeribe and Euphrates formations [26]

4.3 Measurement of Porosity (Φ)

The porosity of reservoir rocks is often determined using porosity logs (Sonic, Density, and Neutron logs).

4.3.1 Sonic Log

Sonic logging is a critical technique for evaluating formations. The sonic tool measures the interval transit time (Δt), or the time in microseconds for an acoustic compressional wave to travel through one foot or meter (μs/ft or μs/m) of formation, along a path parallel to the borehole (reciprocal of velocity). The interval transit time (Δt) is related to primary porosity. With increasing Δt, primary porosity Φ also increases (if other things are constant).

The borehole-compensated (BHC) devices were used in Kor Mor Field and the Wyllie time-average equation [23] (Eq. 3) was utilized.

$$\Phi_S = \frac{\Delta t \log - \Delta tma}{\Delta tfl - \Delta tma} \quad \text{.....Eq. 3.}$$

Where Φ_S is sonic derived porosity, Δt_{ma} is interval transit time in the matrix (Δt limestone or dolomite used, accordingly), Δt_{log} is interval transit time in the formation (measured by log), and Δt_{fl} is interval transit time in the fluid in the formation (salt mud = 185 μsec/ft used in this study).

Both plots of the Δt and Φs curves showed almost a gradational increasing porosity from the top of the Jeribe formation toward the bottom. The porosity at the top of the formation did not exceed 8% and became more than 18% at the bottom due to the increase in dolomitization downward [12]. While the upper part of Euphrates formation had higher sonic porosity exceeding 20% (except a few meters on the top characterized by low porosity), while the porosity of the lower part was around 10% (Fig. 5). Also, the upper part of the Euphrates was more dolomitized than its lower part [12].

4.3.2 Density Log

Density log is a continuous record of bulk density of the formations. The bulk density (ρb) is the density of the entire formation as measured by the logging tool. The formula for calculating density porosity is to determine the density porosity of a formation, either visually or numerically. The matrix density and the type of fluid in the formation must be determined as well [23].

$$\Phi_D = \frac{pma - pb}{pma - pfl} \quad \text{.....} \quad \text{Eq. 4.}$$

Where Φ_D is density derived porosity, ρ_{ma} is the matrix density (in this study 2.71 – 2.88 g/cm^3 were used according to the changes of the lithology from limestone to dolostone), ρb is the formation bulk density (the log reading), ρ_{fl} is the fluid density (salt drilling mud; 1.1 g/cm^{3}used for this study).

The density porosity from both of the Jeribe and Euphrates formations is very variable due to the dolomitized heterogeneity [12], ranging from 1% to 30%, the same as sonic porosity. The upper part of Jeribe had lower porosity than its lower part, while in the Euphrates the density porosity increased upward (Fig. 5).

4.3.3 Neutron Log: Neutron log is used to determine the porosity directly. Its value is proportional to the

amount of hydrogen in the formation, which comes from either hydrocarbons or water trapped in the formation's pores [27].

Figure (6) shows the neutron porosity for Jeribe and Euphrates formations. Since the field is a gas field, the effect of the gas is very clear on both the density and neutron porosities. Gas makes the density porosity overestimated and the neutron porosity underestimated. This effect was treated by calculating the average porosity from both logs, as addressed later through the combination of neutron-density average porosity.

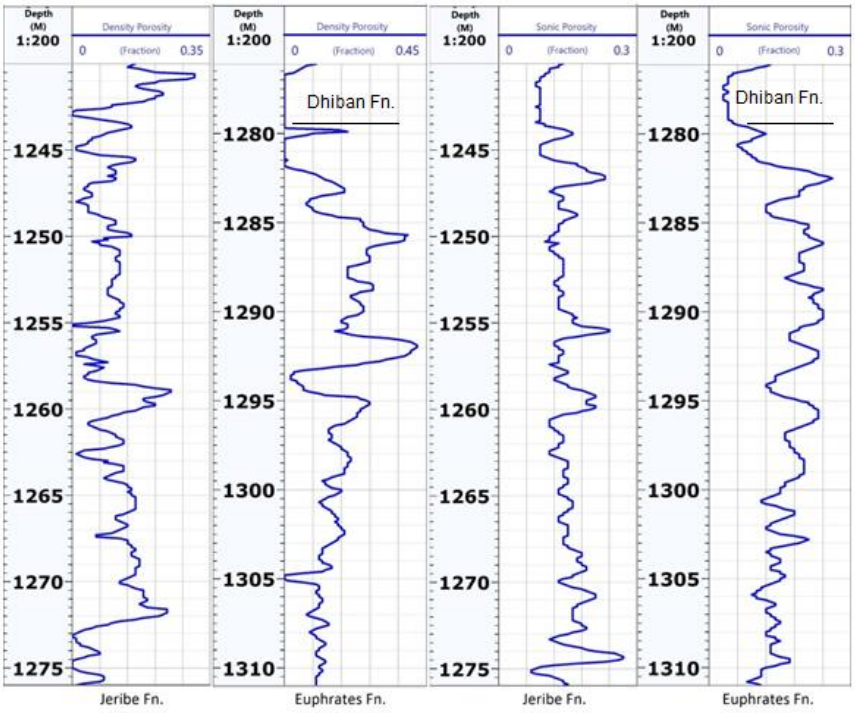

Fig. 5: Sonic and density porosity for Jeribe and Euphrates formations

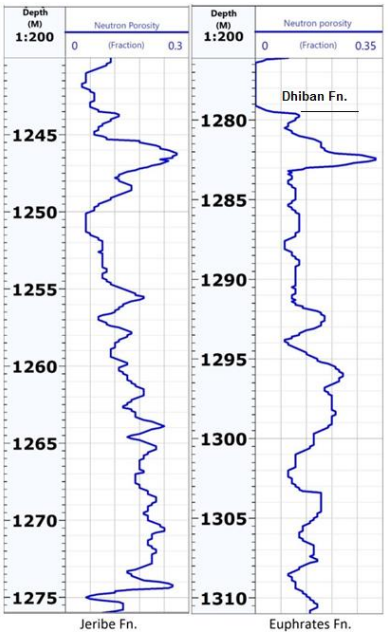

Fig. 6: Neutron porosity for Jeribe and Euphrates formations

4.4 Correction of Porosity from Shale Impact

The presence of shale within the formation affects interpretation of the porosity calculation due to the various properties of shales and the variable reactions of each porosity tool to shale content [28].

All porosity tools (Neutron, Sonic, and Density) would overestimate porosity values in the presence of shale in the formation, and this is true for all common reservoir types (sandstone, limestone, and dolomite reservoirs) [29].

4.4.1 Correcting Sonic Porosity

4.4.1.1 Correcting sonic porosity from shale impact:

$$\Phi S_{corr} = \frac{\Delta tlog - \Delta tma}{\Delta tfl - \Delta tma} - \left(Vsh * \frac{\Delta tsh - \Delta tma}{\Delta tfl - \Delta tma}\right) \ldots \text{Eq. 5 [30]}$$

Where:

ΦS_{corr}: corrected sonic porosity from shale effect

Δt_{log}: interval transit time at any depth

Δt_{ma}: interval transit time of formation's matrix (43.5 to 47.6 µsec/ft for dolomite to limestone used)

Δt_{fl}: interval transit time of fluid (185µsec/ft for salt mud, the case of this study)

V_{sh}: volume of shale at any depth

Δt_{sh}: interval transit time of the adjacent shale (65µs/ft at the depth 1238.3m).

4.4.1.2 Correcting sonic porosity from gas impact:

Also, the sonic porosity was corrected from the gas effect. The interval transit time (Δt) of a formation was increased due to the presence of gas. If the effect of the gas was not corrected as in the case of Kor Mor gas field, the sonic-derived porosity would be too high. Hilchie (1978), as cited in [23], suggested the following empirical corrections for the gas effect:

$\Phi S_{corr} = \Phi S * 0.7$

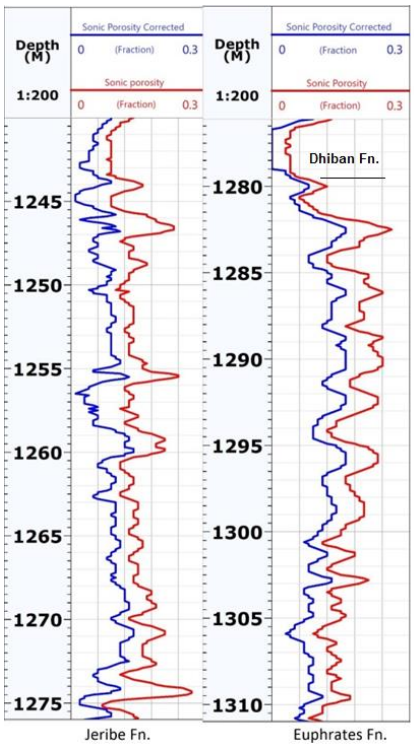

Fig. 7: Corrected sonic porosity from both of the shale and gas effects for Jeribe and Euphrates formations

4.4.2 Correcting Density Porosity

$$\Phi D_{corr} = \frac{\rho ma - \rho b}{\rho ma - \rho fl} - \left(Vsh * \frac{\rho ma - \rho sh}{\rho ma - \rho fl}\right) \ldots \text{Eq. 6. [31]}$$

Where:

ΦD_{corr}: Corrected density porosity from shale effect

ρ_{ma}: Matrix density of the formation

ρ_b: Bulk density at any depth

ρ_{fl}: Fluid density (1.1 gm/cm³ for salt mud, the case of this study)

V_{sh}: Volume of shale at any depth

ρ_{sh}: Bulk density of the adjacent shale (2.55g/c³ at the depth 1238.3m)

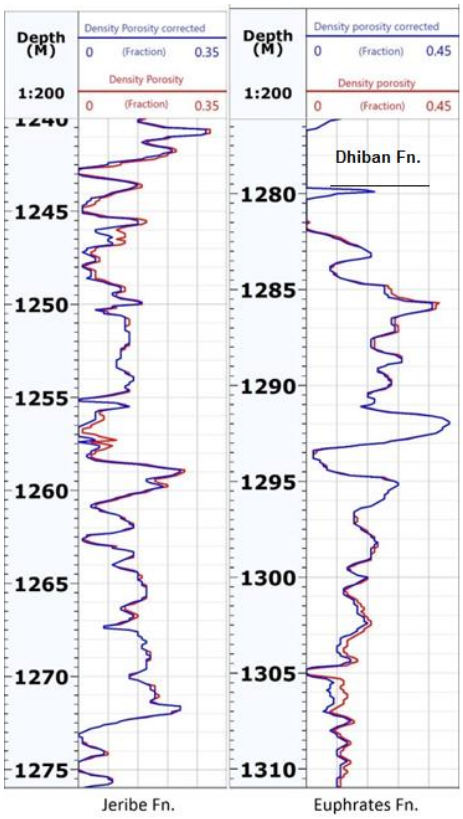

Fig. 8: Corrected density porosity for Jeribe and Euphrates formations

4.4.3 Correcting Neutron Porosity

$\Phi_{Ncorr} = \Phi N - (Vsh * \Phi Nsh)$ …… (Eq.7)

Where:

Φ_{Ncorr}: Corrected neutron porosity from shale effect

Φ_N: Neutron log reading at any depth

V_{sh}: Volume of shale at any depth

Φ_{Nsh}: Neutron porosity for the adjacent shale (0.22 at the depth 1238.3m)

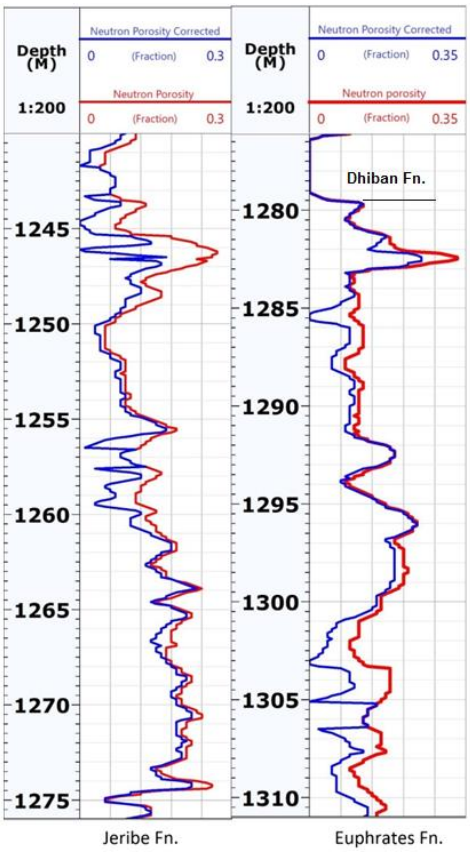

Fig. 9: Corrected neutron porosities for Jeribe and Euphrates formations

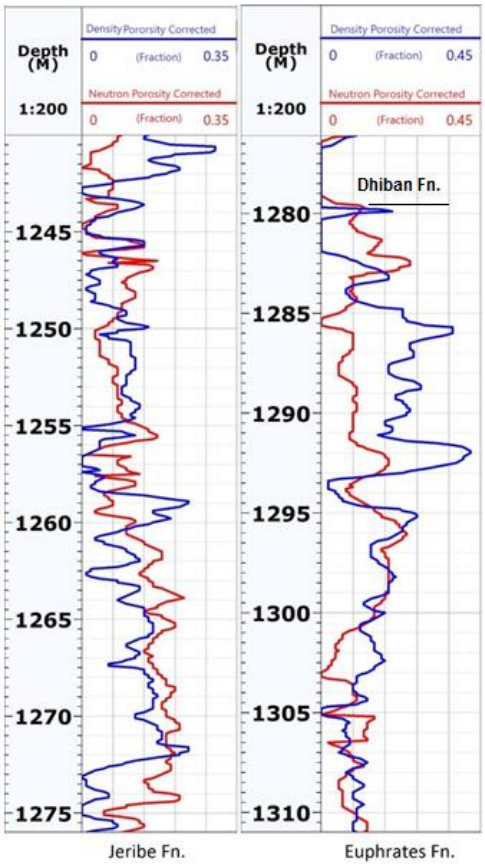

Fig. 10: Corrected neutron-density porosity for Jeribe and Euphrates formations

4.5 Combination of Neutron-Density Porosity Logs (Φ_{ND})

As density and neutron logging tools are typically influenced in different directions by lithological and fluid characteristics, the rate of Φ_D and Φ_N values (referred to as Combination of Neutron-Density Porosity, Φ_{ND}) will be the most dependable and representative recorded porosity at any depth. The porosity of a gas-bearing formation can be estimated by the following equation: [23]

$$\Phi_{ND}gas = \frac{2}{3}\Phi_D + \frac{1}{3}\Phi_N \quad \ldots\ldots\ldots \text{Eq.8.}$$

Where:

$\Phi_{ND}gas$ = porosity of the gas-bearing formation

Φ_N = neutron porosity

Φ_D = density porosity

The effect of gas was evident in the entire reservoir (Fig. 10), where the density porosity was greater than the neutron porosity, excepting for some intervals as this effect was unobserved due to the predominance of dolomite.

4.6 Secondary Porosity (Fracture Index) Detection from Log Data

Within reservoir rocks, two distinct forms of porosity can be identified, namely, primary and secondary. Primary porosity refers to the initial and unique porosity that exists prior to deposition [32]. While secondary porosity is a type of porosity that is generated as a result of the interaction of tectonic forces with formation water. In general, secondary porosity is greater in carbonate rocks than in siliciclastic sediments [33].

The fractures have a great role in improving the reservoir properties (porosity and permeability), especially in carbonate rocks. Therefore, the important portion of the world's hydrocarbon reserves belongs to the fractured carbonate reservoir. The description of the fracture system is the essential petrophysical evaluation of the reservoir.

Sonic log measures the uniform inter-particle or inter-crystalline porosity (primary porosity), while the average measured porosity by neutron-density log is considered as total porosity. When the sonic porosity (Φ_{Scorr}) is compared by using the total neutron and density porosity combination (Φ_{NDcorr}) [Eq. 9]; the difference is found in the secondary porosity (fractures, cavities, vugs ... etc).

$$\Phi_{Sec} = \Phi_{NDcorr} - \Phi_{Scorr} \ldots\ldots\ldots \text{Eq. 9.}$$

Where:

Φ_{Sec}: Secondary porosity

Φ_{NDcorr}: Combination neutron-density porosity (corrected from shale impact and gas)
Φ_{Scorr}: Sonic porosity (corrected from shale impact and gas)
The Jeribe and Euphrates reservoirs in Kor Mor field showed a reasonable high secondary porosity (Fig. 11, green color), making a significant fraction in both Jeribe and Euphrates units represented by 20% and 27% of the total porosities, respectively.

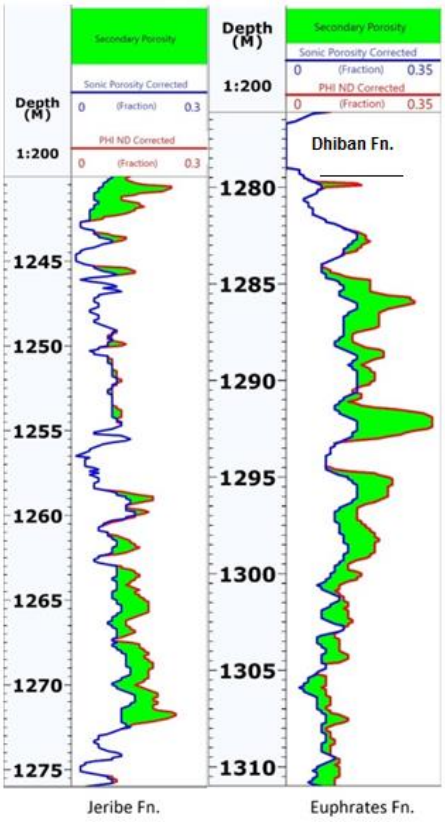

Fig. 11: N-D combination and secondary porosity for both Jeribe and Euphrates formations

The majority of the secondary porosity was related to the Euphrates unit, ranging between 0% and 19%, and the upper and lower part of the Jeribe reservoir, ranging between 0% and 15% (Fig. 11). This resulted in a complete mud loss in these two units during the drilling process. Hence, lost circulation material (LCM) had to be used, along with decreasing the mud weight in order to control the situation [12].

5. Conclusions

This study revealed the following conclusions:
1. Both formations (Euphrates and Jeribe) have different thicknesses all over the field. The thickness of the Euphrates formation ranges from 30 to 65 m, and Jeribe formation from 30 to 50m. The two formations are separated by an anhydrite Dhiban formation with a thickness of 3 to 10 m in the drilled wells.
2. The upper part of the Jeribe formation is mostly limestone and its lower part is characterized by dolostone; whereas the dolomitization is more complete in the upper part of the Euphrates formation.
3. The Jeribe formation comprises two shaly intervals in its upper and middle parts, while the Euphrates includes a shaly interval in the lower part and some bands in the upper part
4. Porosity of the Euphrates reservoir ranges between 0.0 and 0.33 with an average of 0.15, and the Jeribe reservoir ranges between 0.01 and 0.23 with an average of 0.10.
5. The secondary porosity makes a significant fraction of porosity in both units. In Euphrates reservoir, it ranges between 0 and 0.19; whereas in Jeribe reservoir, it ranges between 0 and 0.15. This quantity represents 0.20 to 0.27 of the total porosities. These fractures are resulted in a complete mud loss from some intervals in these two units during the drilling process.

6. References

[1] Al-Sakini, J.A., 1992. Summary of petroleum geology of Iraq and the Middle East: Kirkuk. Northern Oil Company Press, Iraq (in Arabic, p 179).
[2] Al-Ameri, T.K., Zumberge, J. and Markarian, Z.M., 2011. Hydrocarbons in The Middle Miocene Jeribe Formation, Dyala Region, NE Iraq. Journal of Petroleum Geology, 34(2), pp.199-216.
[3] Hussein, D.O., 2015. Reservoir characterization of ramp carbonates: Lessons from the Lower Miocene Euphrates and Jeribe Formations, Kurdistan, N. Iraq (Doctoral dissertation, University of Leeds).
[4] Baban, D. and Hussein, H.S., 2016. Characterization of the Tertiary reservoir in Khabbaz Oil Field, Kirkuk area, Northern Iraq. Arabian Journal of Geosciences, 9(3), pp.1-19.
[5] Hussein D, Collier R, Lawrence J, Rashid F, Glover P, Lorinczi P, Baban D (2017) Stratigraphic correlation and paleoenvironmental analysis of the hydrocarbon-bearing Early Miocene uphrates and Jeribe formations in the Zagros folded-thrust belt. Arab J Geosci 10:543
[6] Saeed, M. B. 2017. Reservoir Characterization of The Jeribe Formation (Middle Miocene) From Selected Wells in Hamrin Oil Field, Northern Iraq (Msc. Dissertation, University of Sulaimani)
[7] Abdullah H G., & R. E. L. Collier & N. P. Mountney(2019), The palaeoshoreline of Early Miocene formations (Euphrates and Jeribe) at the periphery of the Zagros Foreland Basin, Sulaimani Governorate, Kurdistan Region, NE Iraq. Arabian Journal of Geosciences (2019) 12: 574.
[8] Fadhil, D.T., Yonus, W.A. and Theyab, M.A., 2020. Reservoir characteristics of the Miocene age formation at the Allas Dome, Hamrin Anticline, Northern Iraq. MMD J, 14, pp.17-23.
[9] Abdulrahman Salam S., Manal S. Al-Kubaisi and Ghazi H. Al-Shara'a, 2020. Formation Evaluation for

Jeribe Formation in the Jaria Pika Gas Field. Iraqi Geological Journal, 53 (2F), 2020: 83-93

[10] Deabl, R.A., Ramadhan, A.A. and Aldabaj, A.A., 2021. Evaluation of Petrophysical Properties Interpretations from Log Interpretation for Tertiary Reservoir/Ajeel Field. Iraqi Journal of Oil & Gas Research, 1(1).

[11] Addendum to Geological Appraisal Well (Km-9) on the Kor Mor Structure, Zagros Fold Belt, Kurdistan Region, Iraq 2008.

[12] Km-9 Final well report, Dana Gas , 2009.

[13] Buday, T. and Jassim, S.Z., 1987. The Regional geology of Iraq: Tectonism Magmatism, and Metamorphism. II Kassab and MJ Abbas. Baghdad, 445.

[14] Mohialdeen, I.M., Fatah, S.S., Abdula, R.A., Hakimi, M.H., Abdullah, W.H., Khanaqa, P.A. and Lunn, G.A., 2022. Stratigraphic Correlation and Source Rock Characteristics of the Baluti Formation from Selected Wells in the Zagros Fold Belt, Kurdistan Region, Northern Iraq. Journal of Petroleum Geology, 45(1), pp.29-56

[15] Iraq Development potential, 2003. Iraq Field Atlas part2 (p30, 118).

[16] Aqrawi AA, Horbury A, Sadooni F (2010) The Petroleum Geology of Iraq. Wiley Online Library, Beaconsfield

[17] Jassim, S. Z., and M. Al-Gailani (2006) ″ Chapter 18: Hydrocarbons″ in Geology of Iraq, (1st ed.), Edited by Jassim S. Z., and Goff J. C. PP. 169-184. Brno, Czech Republic: Dolin, Prague and Moravian Museum

[18] Bellen, R.C. van, Dunnington, H.V., Wetzel, R. & Morton, M. (eds.), (1959) "Lexique stratigraphic international", Paris, v. III, Asie, Fascicule 10a Iraq. 333 p.

[19] Prazak, J., 1974. Stratigraphy and paleontology of the Miocene of the Western Desert, W. Iraq. Manuscript report, GEOSURV, Baghdad.

[20] De Böckh, H., Lees, G. M., and Richardson, F. D. S., 1929. The Structure of Asia (edited by Gregory, J. W.), chapter iii and Postscript.

[21] Rider, M H., 2002, The geological interpretation of well logs, 2nd edition. Rider-French Consulting Ltd, pp.280

[22] Larionov, V.V., 1969. Radiometry of boreholes. Nedra, Moscow, 127p.

[23] Asquith, G.B., Krygowski,. 2004. Basic well log analysis (Vol. 16). Tulsa: American Association of Petroleum Geologists.

[24] M. Ghorab, Mohmed A.M. Ramadan and A.Z. Nouh. 2008. The Relation Between the Shale Origin (Source or non Source) and its Type for Abu Roash Formation at Wadi El-Natrun Area, South of Western Desert, Egypt. Australian Journal for Basic and Applied Sciences, 2(3), p.360.

[25] Erin M. Mcgowan, 2015. Spectral Gamma Ray Characterization Of The Elko Formation, Nevada-A Case Study For A Small Lacustrine Basin. Master Thesis, Department of Geosciences, Colorado State University, Fort Collins, Colorado.

[26] Schlumberger (2009) "Log Interpretation Charts". Sguard Land, Texas.

[27] Brown, S.J. (1963) Handbook of Well-Log Analysis for Oil and Gas Formation Evaluation: Printice-Hall International Incorporated, London, p.21.

[28] Bassiouni, Z., 1994. Theory, measurement, and interpretation of well logs (Vol. 4, p.372). Dallas, TX, USA: Henry L. Doherty Memorial Fund of AIME, Society of Petroleum Engineers.

[29] Asquith, G.B. and Gibson, C.R., 1982. Basic well log analysis for geologists (Vol. 3). Tulsa: American Association of Petroleum Geologists.

[30] Dewan, J.T., 1983. Essentials of modern open-hole log interpretation: PennWell Publishing Company, Tulsa, Oklahoma, 361 p.

[31] Schlumberger, D., 1972. Vorôd l'agoranome. Syria, pp.339-341.

[32] Choquette, P.W. and Pray, L.C., 1970. Geologic nomenclature and classification of porosity in sedimentary carbonates. AAPG bulletin, 54(2), pp.207-250.

[33] Heinemann, Z. and Mittermeir, G., 2013. Fluid flow in porous media. The Textbook series of the PHDG is an aid for PhD students. Roseggerstr. E-Mail: phdg@a1.net

الخواص المكمنية للتكاوين الجيرية ذات العمرمايوسين الاسفل فى حقل كورمور الغازي، منطقة كركوک، شمال شرق العراق

فؤاد محمد قادر ، شاباز محمد علي

قسم علم الارض، كلية العلوم ، جامعة السليمانية ، السليمانية ، العراق

الملخص

تم اختيار التقييم المكمني لتكوينين الجيريين؛ الفرات، والجيريبي (الميوسين الاسفل) في حقل كور مور الغازي في شمال شرق العراق. تراوحت سماكة تكوين الفرات بين 30 و 65 و الجريبي بين 30 و 50 مترا في هذا الحقل ، وتعلوهما طبقة غطاء متبخرات سميكة من تكوين الفتحة. وكما تفصل التكوينين بواسطة طبقة رقيقة من صخور المتبخرات لتكوين الذبان. تم استخدام المجموعة الكاملة من بيانات المجسات للبئر (Km-9) بالاضافة الى القراءات المتوفرة لثمان آبار الاخرى من Km-1 الى Km-8، ومن نتائج التحاليل للبيانات فى تقييم خصائص المكمنية للوحدتين، ظهرت ان فى الغالب كلا من دولوستون والحجر الجيري الدولوميتى كانا صخاريتين مهيمنتين فى هذين التكوينين. و من بيانات المجسات ، تم تقدير أنواع مختلفة من الخصائص المكمنية متمثلا بمحتوى الطين ، أنواع الطين ، المسامية الاولية ، والمسامية الثانوية (الكسور، الشقوق، ولفجوات).